M. F. Horstemeyer

J. Lim

W. Y. Lu

Center for Materials and Engineering Sciences,
Sandia National Laboratories,
Livermore, CA 94551-0969

D. A. Mosher
UTRC MS129-73,
411 Silver Lane East, East Hartford, CT 06108

M. I. Baskes
MST-8, Los Alamos National Laboratory,
Los Alamos, NM 87545

V. C. Prantil
Milwaukee School of Engineering,
Mechanical Engineering Department,
S229, Milwaukee, WI 53202-3109

S. J. Plimpton
Sandia National Laboratories,
Albuquerque, NM 87185-5800

Torsion/Simple Shear of Single Crystal Copper

We analyze simple shear and torsion of single crystal copper by employing experiments, molecular dynamics simulations, and finite element simulations in order to focus on the kinematic responses and the apparent yield strengths at different length scales of the specimens. In order to compare torsion with simple shear, the specimens were designed to be of similar size. To accomplish this, the ratio of the cylinder circumference to the axial gage length in torsion equaled the ratio of the length to height of the simple shear specimens (0.43). With the [110] crystallographic direction parallel to the rotational axis of the specimen, we observed a deformation wave of material that oscillated around the specimen in torsion and through the length of the specimen in simple shear. In torsion, the ratio of the wave amplitude divided by cylinder circumference ranged from 0.02–0.07 for the three different methods of analysis: experiments, molecular dynamics simulations, and finite element simulations. In simple shear, the ratio of the deformation wave amplitude divided by the specimen length and the corresponding values predicted by the molecular dynamics and finite element simulations (simple shear experiments were not performed) ranged from 0.23–0.26. Although each different analysis method gave similar results for each type boundary condition, the simple shear case gave approximately five times more amplitude than torsion. We attributed this observation to the plastic spin behaving differently as the simple shear case constrained the dislocation activity to planar double slip, but the torsion specimen experienced quadruple slip. The finite element simulations showed a clear relation with the plastic spin and the oscillation of the material wave. As for the yield stress in simple shear, a size scale dependence was found regarding two different size atomistic simulations for copper (332 atoms and 23628 atoms). We extrapolated the atomistic yield stresses to the order of a centimeter, and these comparisons were close to experimental data in the literature and the present study.
[DOI: 10.1115/1.1480407]

Introduction

Pure FCC Cu has enjoyed a breadth of mechanical property studies. Polycrystalline Cu studies have been performed in torsion (cf., Shrivastava et al. [1]; Johnson et al. [2]; Montheillet et al. [3]; Canova et al. [4]; Field and Adams [5]; Horstemeyer and McDowell [6]), tension (cf., Khan and Parkh [7]), compression (cf., Hecker et al. [8], Horstemeyer and McDowell [6]; Butler et al. [9]; Tanner and McDowell [10]), and non-monotonic path sequences (cf., Yakou et al. [11]; Khan and Parikh [7]; Franciosi et al. [12]; Khan and Wang [13]; Tanner and McDowell [10]). For single crystal Cu, [14], Phillips [15], Jackson and Basinski [16], Honeycombe [17], and Quilici et al. [18] have noted critical resolved shear stresses under various loading conditions. Even boundary value problems with single crystal copper have been performed. For example, a high strain rate analyses/experimental study with the single crystal oriented for planar double slip by Rashid et al. [19]. Although single crystal Cu compression and tension tests have been conducted, few torsion and simple shear tests have been conducted. In this work, we perform torsion tests of solid bars of single crystal Cu. Historically, little research has been presented with this type of test for several reasons. First, it is a difficult test to achieve accurate load-rotation responses. In this paper, we describe how our method yields repeatable responses. Second, researchers typically use compression or tension tests to determine the yield stress. Third, researchers typically used thin-walled torsion tests to achieve large strains and avoid stress gradients that require plasticity analysis. By performing the single crystal solid bar torsion test with a ''minimal'' amount of dislocations present, we show qualitatively the effects of dislocation nucleation on the yield point.

A second aspect of this investigation is related to atomistic simulations. The single crystal torsion experiments are compared to single crystal simple shear and torsion simulations using molecular dynamics (MD) in an effort to analyze the phenomenological behavior. Horstemeyer and Baskes [28] performed simple shear MD simulations using embedded atom Method (EAM) potentials for single crystal Ni but in this study an EAM potential is used for single crystal Cu (Foiles [21]) at two different size scales.

A third aspect of this investigation includes a finite element simulation using a crystal plasticity model (Horstemeyer et al. [20]) of a single Cu crystal oriented in the same manner as the experiments and atomistic simulations. The crystal plasticity simulation of the torsion cylinder was used to relate the phenomenological behavior with the experiments and atomistic simulations.

To the authors' knowledge, the examination of the kinematics and stress response by using a combination of physical experiments, MD simulations, and crystal plasticity finite element simulations for torsion/simple shear of single crystal Cu has not been performed. One might ask why such a study is necessary. This type of study can serve a dual purpose: to relate microstructural mechanisms to mechanical properties and help guide continuum modeling at various scales. In particular, the experiments, MD simulations, and crystal plasticity finite element simulations provide different and unique perspectives and understanding of torsion/simple shear that when synergized generate a clear picture of the cause-effect relations of the microstructure-property relations. Experiments give the stress-strain response and material rotation phenomena but cannot provide the understanding of the mechanisms. It is the crystal plasticity finite element simulations and MD simulations that provide the understanding of the mecha-

Contributed by the Materials Division for publication in the JOURNAL OF ENGINEERING MATERIALS AND TECHNOLOGY. Manuscript received by the Materials Division April 11, 2001; revised manuscript received December 11, 2001. Guest Editors: Tariq A. Khraishi and Hussein M. Zbib.

nisms of the plastic spin and dislocation nucleation and interaction. The crystal plasticity formalism starts at the scale of the crystal grain but does not inherently include subgrain division or much about substructures within grains. As such, crystal plasticity can provide information regarding the plastic spin with respect to the stress-strain response and rotations but not about the mechanisms related to detailed dislocation nucleation and interaction effects. The MD simulations are limited to small sizes and high applied strain rates but provide the mechanistic observations needed to relate the dislocation nucleation and interaction with the plastic spin and stress-strain responses at the higher scales. Furthermore, when combining these three independent methods, the similarities and differences between torsion and simple shear become clearly delineated.

Experiments

Two Cu single crystal bars with 99.999% purity were grown from a seed. The diameter of the specimens was 12.7 mm and the length was 50 mm with a ⟨110⟩ crystallographic direction parallel to the axial direction of the specimen. This orientation allowed for quadruple slip. Referring to Fig. 1, in order to clamp the specimen to the torsional testing machine, each end of the specimen was epoxied inside an aluminum end cap. Figure 2 shows that the aluminum end caps were then clamped to a MTS multiaxial test system with one end clamped to the torque cell and the other end to the torsional actuator. The effective gage length of the specimen then became 17.6 mm.

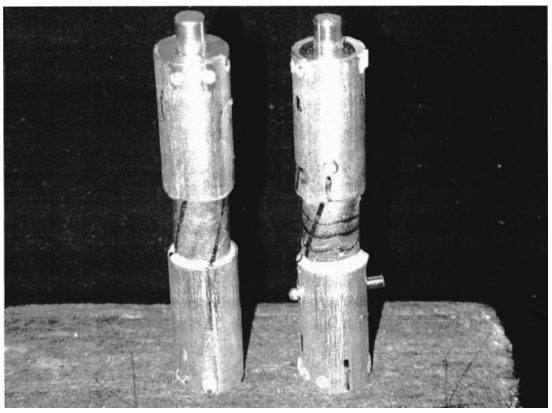

Fig. 1 Pictures of two single Cu crystal torsional specimens

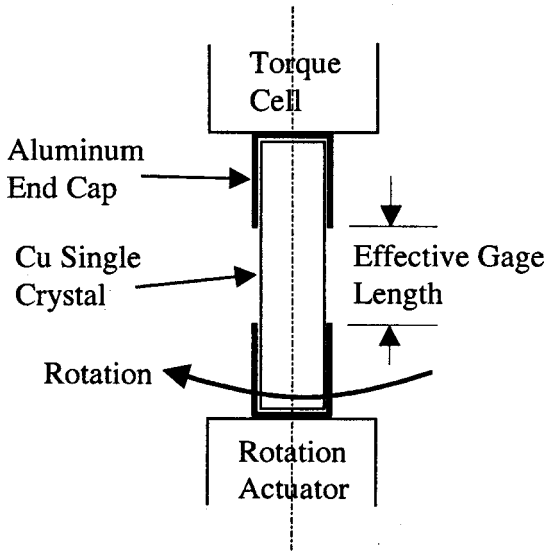

Fig. 2 Schematic of MTS multiaxial test system

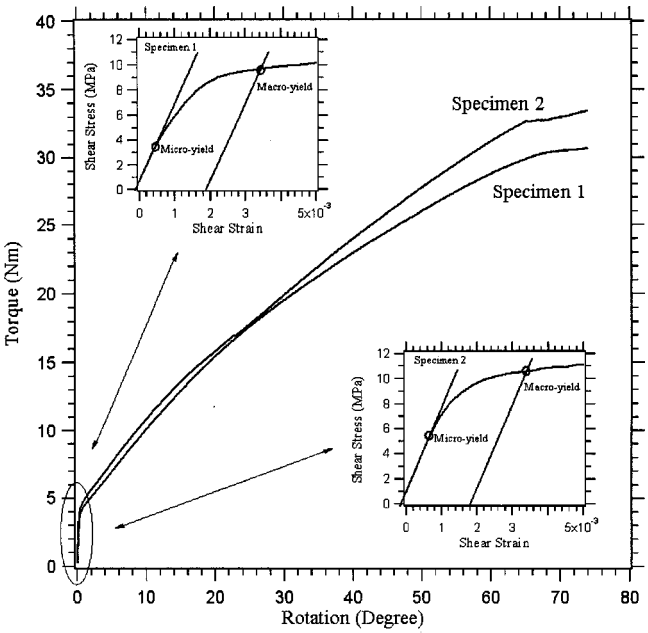

Fig. 3 Torque-rotation curves for two different single crystal Cu specimens that had an axial orientation in the [110] direction

Rotations were applied by the torsional actuator at a rate of 0.25°/s. The torque-rotation curves of two different specimens (1 and 2) are plotted in Fig. 3. The stress state can be accurately calculated using an elastic analysis at yield but becomes more inaccurate as the deformation proceeds into the plastic regime. As such, we quote only stresses using the elastic formula near yield. Both curves in Fig. 3 show that Cu single crystal yields at a very low stress level (near 10 MPa) but the work hardening rate after yield is very high. In the context of this writing, we define two yield points. Macroyield is defined from the 0.2% strain offset. Microyield is defined at the proportional limit, when deviation from linearity starts. Table 1 shows the microyield and macroyield values for the two specimens. The stress values in Table 1 were evaluated at the outer radius of the specimen since the specimens experienced a stress gradient as the deformation proceeded.

An observation related to the kinematics of deformation on the outside surface of the specimen was made. As evidenced in Fig. 4 from the machining marks on the surface of the specimens, a wavy deformation pattern developed around the circumference during torsion. These machining marks were initially straight before torsion. The sinusoidal wave comprises of four periods believed to result from the fourfold symmetry of the dislocation glide planes around the circumference with an average ''amplitude'' of approximately 0.35 mm at the center of the gage section. This wavy periodic deformation is shown in Fig. 4 at a strain level of 35%.

Table 1 Yield values of the torsion specimen

Specimen #	Microyield	Macroyield
1	3.5 MPa	9.8 MPa
2	4.8 MPa	10.6 MPa

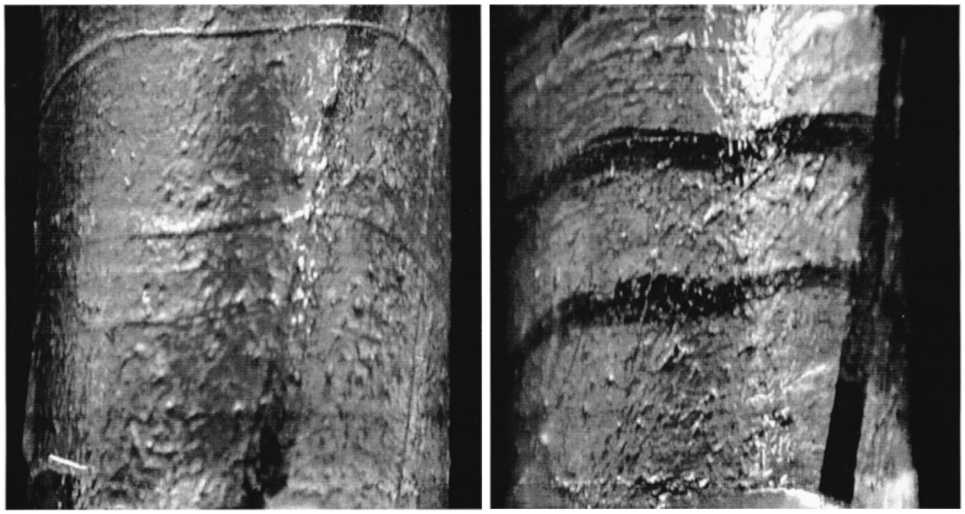

(*a*) (*b*)

Fig. 4 Close-up view of specimens at 35% shear strain illustrating wavy pattern on outside of bar

Atomistic Analysis

Atomistic calculations have been used for a wide variety of materials. All start from atomic pair potentials or some related modification. Brenner [22] summarized the class of bond order formalism which has proven valuable for covalently bonded systems. Stoneham et al. [23] summarized the shell model, which is a modification of a pair potential, used for ceramics. Daw and Baskes developed the Embedded Atom Method (EAM), which employs a pair potential augmented by a function of another pairwise sum, for metals. We used EAM potentials (Daw and Baskes [24]; Daw et al. [25]; Angelo et al. [26]; Baskes et al. [27]) for single crystal Cu (Foiles [21]). Table 2 summarizes the simulation parameters.

Molecular dynamics (MD) simulations of single crystal Cu were performed under fixed-end simple shear and torsion boundary conditions to give insight into the torsional experiments described earlier. Strictly speaking, simple shear requires that the traction-free face of the continuum point remain planar and parallel. We loosen that requirement to analyze potential inhomogeneous deformation predicted by our chosen modeling frameworks. Our ultimate goal was to examine simple shear experiments, which do not constrain the x-faces to be planar and parallel (see Fig. 5).

The simple shear simulation had free surfaces in the *x*- and *y*-directions with periodicity in the z-direction as shown in Fig. 5. The aspect ratio (x/y) of the atomistic simulations was identical to the ratio of the circumference to gage length of the torsion specimen. For simple shear, the atoms in the top row in the *y*-direction were prescribed to move in the *x*-direction and the bottom row of atoms was fixed. For the torsion simulation the computational block of material was fixed on one end with a rotation prescribed at the other end, also shown in Fig. 5. An applied strain rate of ~1e9/s was used for both types of simulations. A full discussion of strain rate effects can be found in Horstemeyer et al. [28]. The high applied strain rate arises because a femtosecond (10^{-15} s) time step is needed to resolve dynamic simulation equilibrium. Hence, large simulation times are not possible. As a result, high strain rates are needed to reach large strains. A constant periodic length, a fixed number of atoms, and temperature of 300 K were used for the material that was oriented initially for quadruple slip. No initial defects were introduced into the material. An initial velocity in the *x*-direction scaled according to the height (*y*-direction) was introduced to alleviate a potential shock. The interior atoms were used to determine the average stress of the specimen. Figure 6 shows the relative displacement results from a simulation at 35% shear strain under simple shear. Similarly, Fig. 7 shows relative displacement results from the hollow and solid cylinder simulations at 35% shear strain under torsion. The vectors show the relative displacements from the original positions. One can see that the sinusoidal

Table 2 Summary of information regarding specimen geometries and test conditions

Attribute	Experiment	Atomistics	Atomistics	Atomistics
	solid cylinder	solid cylinder	hollow cylinder	simple shear
number of atoms	-	46,619	15,210	23,628
length (x-dir)	-	-	-	250 Å
height (y-dir)	17.6 mm	108 Å	108 Å	108 Å
depth (z-dir), periodic	-	40 Å	7 Å	7 Å
radius	6.35 mm	40 Å	40 Å	-
aspect ratio	2.27	2.33	2.33	2.31
loading condition	torsion ⟨110⟩	torsion ⟨110⟩	torsion ⟨110⟩	simple shear ⟨100⟩
applied strain rate	10^{-3} s^{-1}	10^{9} s^{-1}	10^{9} s^{-1}	10^{9} s^{-1}
crystal orientation	$(001,110,1\bar{1}0)$	$(001,110,1\bar{1}0)$	$(001,110,1\bar{1}0)$	$(001,110,1\bar{1}0)$

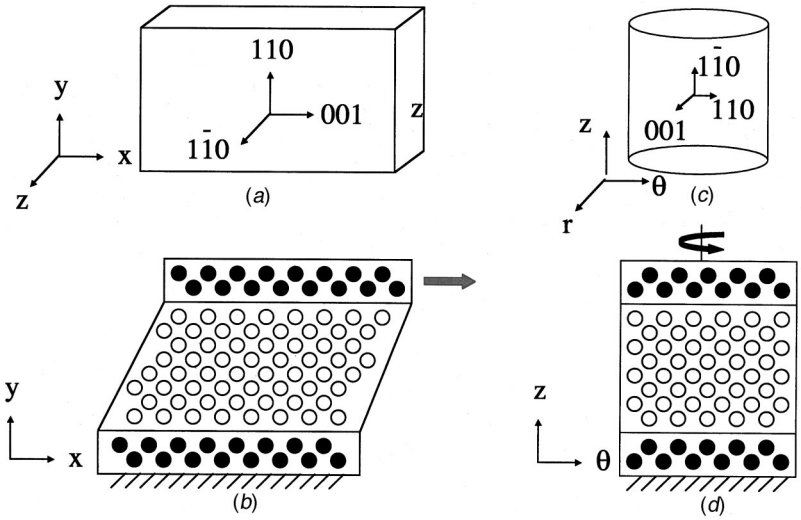

Fig. 5 Schematic of simulation block of atoms for (*a*) simple shear initial state, (*b*) simple shear at large strain, (*c*) torsion initial state, and (*d*) torsion at large strain in which the clear circles represent the active atoms and dark circles represent the boundary atoms

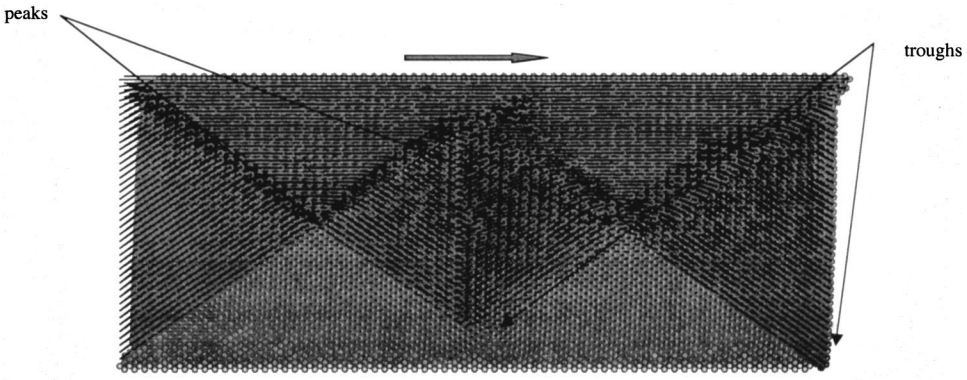

Fig. 6 Plot of atoms showing relative displacements from original positions for a specimen under simple shear

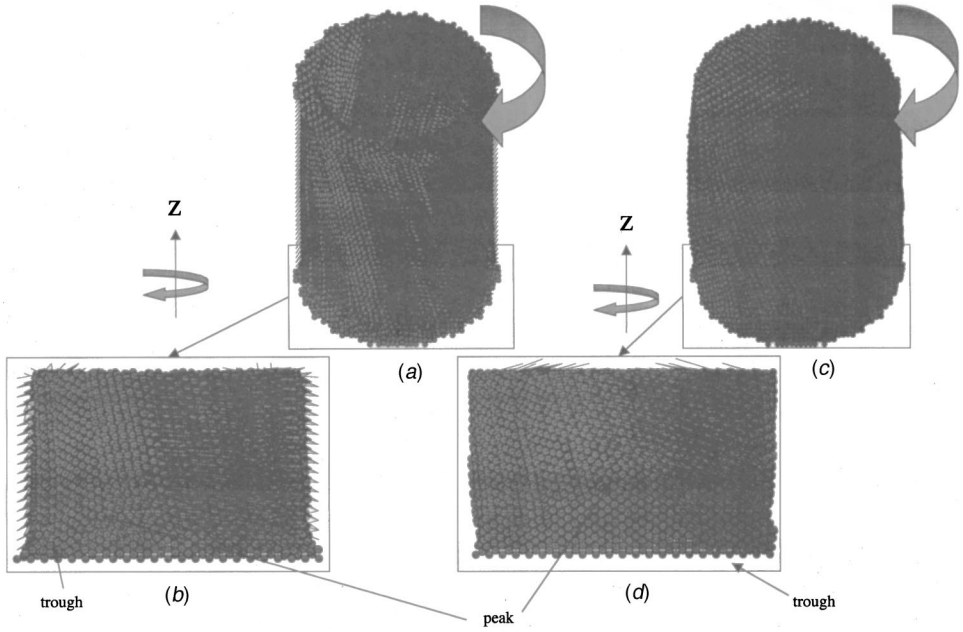

Fig. 7 Plot of atoms showing relative displacements from original positions for (*a*) hollow cylinder and (*b*) solid cylinder under torsion. Lines show relative displacements

wave observed in the torsional experiment is also observed here in both types of simulations. One thing is clear: that dislocations are emitted from the corners of the block of material (cf. Horstemeyer and Baskes [29]). After the dislocations are nucleated, they propagate into the interior of the block of material and the oscillatory deformation pattern results.

To determine the yield stress of the atomistic simulation specimens, a volume average of the shear component dipole force tensor (cf., Horstemeyer and Baskes [29]) is used. The simple shear atomistic simulation showed that the microyield and macroyield stresses from the atomistic simulations were 1.95 and 3.1 GPa, respectively. The determination of a yield stress was difficult to determine for a torsion atomistic simulation because a stress gradient exists with respect to the radial distance. If one considers just the outside cylinder perimeter (same as the experiments), two problems arise: (1) the boundary conditions are prescribed by a thermal velocity and in doing so, the force determination is inappropriate to use for a stress calculation, and (2) surface atoms cannot be expected to yield bulk effects because of the large volume-to-surface area. Hence, in this study we simply use the simple shear yield stress values.

Finite Element Analysis With Crystal Plasticity

Finite element simulations employing a crystal plasticity constitutive model (cf, Cuitino and Ortiz [30], Horstemeyer et al. [20]) within ABAQUS (Hibbitt et al. [31]) was used to give insight into the underlying substructural physical mechanisms possibly responsible for the deformations related to the oscillatory pattern observed on the outside surface of the experimental torsion specimen. The crystal orientation, rotational rate, gage length, and diameter were the same as the experiment. Note that there is no inherent size scale in these calculations. A simple shear simulation was also performed with the corresponding geometry. Results for these simulations were almost identical when single Gauss point elements and higher order elements were used. For the simple shear simulation, elements had an initial aspect ratio of one-to-one with fifteen elements aligned vertically and thirty elements aligned horizontally. A mesh refinement study of doubling both sides showed no quantitative differences in the results. For the torsion simulations, eight elements were used with a one-to-one aspect ratio through the diameter, and sixteen elements were aligned through the specimen length. No mesh refinement study was performed.

Figures 8 and 9 show the relation of one of the Euler angles and the relative displacement of the material at large strain under simple shear and torsion, respectively. For the simple shear case, note that two peaks are observed in the specimen (Fig. 8(*b*)) and this arises because of the plastic spin drives crystal reorientation (Fig. 8(*a*)). For the torsion simulation shown in Fig. 9, we observe that rotation angles are of opposite sign on opposite sides of the specimen. On the left hand side, we see a peak clockwise (CW) rotation and on the right hand side, we see a peak counterclockwise (CCW) rotation. These opposing rotations push material up and down in the specimen to induce the oscillatory deformation pattern. Note that the minimum and maximum rotation angles correlate with the peaks and troughs of the displacement oscillations.

Discussion

We now discuss the similarities and differences in the experiments, molecular dynamics simulations, and finite element simulations. First, we will discuss the oscillatory deformation pattern observed on the outside circumference of the specimen and then differences in the kinematics and in micro/macro-yield (stress) response. Before we make comparisons though, we must first clarify a point regarding simple shear and torsion. If one assumes that the curvature related to the circumferential normal strain is negligible, then the stress response in simple shear and torsion is the same from a continuum perspective. In moving from the cylindrical coordinate system for torsion to the Cartesian coordinate system for simple shear the coordinates r, θ, z map to z, x, y, respectively. Note then that in the torsion experiments and simulations, the free surface is the θz plane, but the free surface in the simple shear simulations is the zy plane.

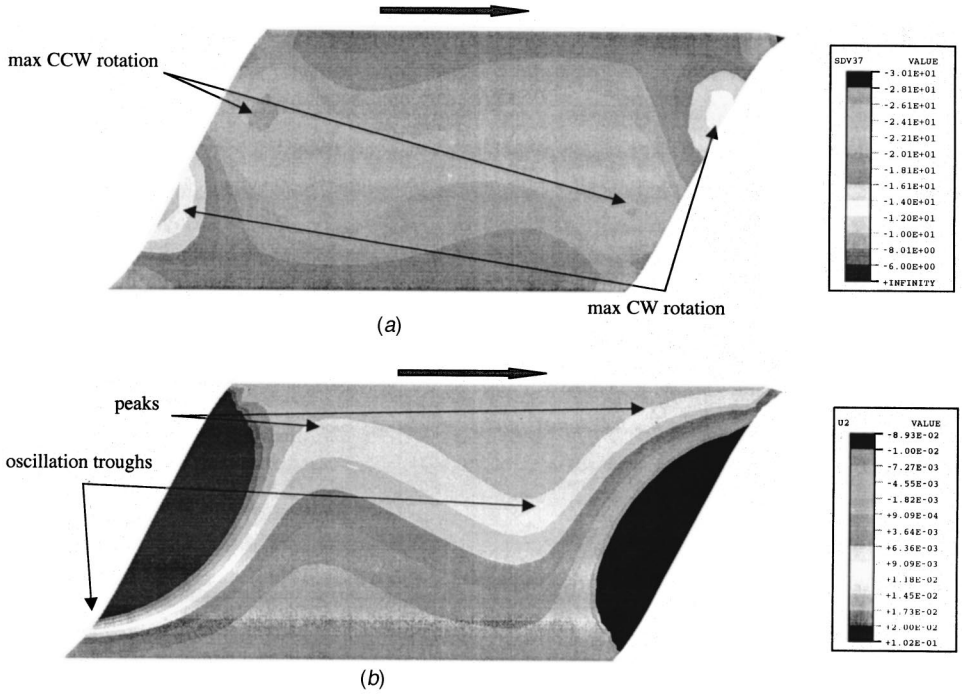

Fig. 8 Finite element simulation of single crystal Cu showing (*a*) one Euler angle and (*b*) the correlating displacements to illustrate the oscillating pattern in simple shear

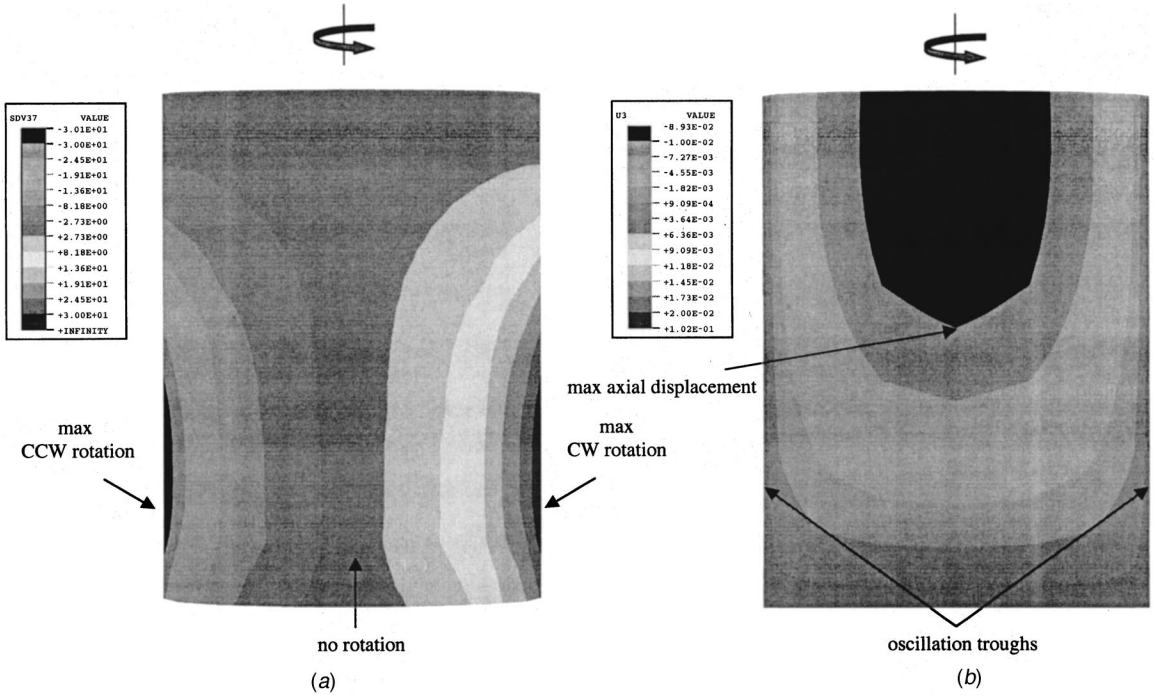

Fig. 9 Finite element simulation of single crystal Cu showing (*a*) one Euler angle and (*b*) the correlating displacements to illustrate the oscillating pattern in torsion

Kinematics and Deformation. The main similarity observed in all the simulations and experiments was an oscillatory deformation pattern that was observed on the outer surface of the specimen. The oscillatory pattern occurred because the kinematics are qualitatively the same in the MD, finite element simulations, and experiments. However, the magnitude and period of the oscillating waves are different in simple shear and torsion. This arises because the cubic symmetry of the FCC crystal and the symmetry of the loading are not identical, since the θz shear plane changes orientation around the circumference of the specimen. The finite element simulation shows this in Figs. 8 and 9. For the torsion case (experiments, MD simulations, and finite element simulations), four peaks were observed, but in the simple shear case (MD simulations and finite element simulations) only two peaks were observed. The differences between torsion and simple shear were also observed by Boukadia and Sidoroff [32] but at much larger strains. In this study, the four peaks in the torsion and two peaks in the simple shear start to develop at the beginning of the deformation. This reflects the fourfold slip activity revealed in the torsion experiment and planar double slip exhibited in the simple shear simulations. These two types of slip activity clearly reflect that the plastic spin operates differently when comparing simple shear to torsion.

Not only are the number of periods different between torsion and simple shear, but the wave amplitudes were also different when we compare the ratio of the wave amplitude divided by the cylinder circumference for torsion and length for simple shear. We kept the ratio of the circumference of the cylinder to the axial gage length of the torsion equal to the ratio of the length to height in the atomistic simulation (0.43). Similarly, we kept the same ratio for simple shear when comparing the length-to-height. Table 3 shows a comparison of the wave amplitude ratios at 35% strain. The peak and trough values are readily determined in the experiment, whereas these values need to be considered only approximate for the MD simulations and finite element simulations. Note that both the torsion wave amplitude ratio and simple shear wave amplitude ratio were consistent within their own domains, but different when comparing torsion to simple shear. For torsion, the wave amplitude was much smaller than in simple shear. This difference may have to do with either the differences in plastic spin related to slip activity as discussed earlier or related to different free surfaces in each type of boundary condition. Although both have traction free planes orthogonal to the loading direction, the planes are opposite to the coordinate mapping from a cylindrical to the Cartesian coordinate system as r, θ, z map to z, x, y, respectively.

If torsion and simple shear were identical, the θz plane in torsion would map to the xy plane in simple shear. The θz plane in torsion is traction free, but the xy plane is not traction free but is constrained by periodic conditions. The yz plane in simple shear is traction free.

Table 3 makes three points. (1) Simple shear and torsion boundary conditions incur different kinematics as expressed by the wave amplitude ratio. (2) The wave amplitude is very similar in torsion for the experiments, finite elements, and atomistic simulations, although there is minor variation within the different methods. The difference between the hollow and solid cylinders for the atomistic simulations may be due to the extra internal surface to allow dislocation nucleation for the hollow cylinder. Also, there exists a difference between the crystal plasticity simulation and the experiment from 0.02 to 0.05, respectively, even though these two simulations are considered to be on the same scale. The difference could arise for several reasons, but the main one is probably that the crystal plasticity formulation does not explicitly

Table 3 Ratio of wave amplitude divided by circumference (torsion) or length (simple shear) of different boundary conditions and methods at large strain

Condition/method	Wave amplitude ratio
Torsion	
experiment	0.02
finite elements	0.05
molecular dynamics (solid cylinder)	0.06
molecular dynamics (hollow cylinder)	0.025
Simple shear	
finite elements	0.25
molecular dynamics	0.23

account for substructural development that is observed in finite deformations. (3) The simple shear wave amplitude ratio is essentially the same for the finite element simulations and the atomistic simulations. This result reveals that no specimen size scale effect exists related to the kinematics in torsion.

Stress Response. When comparing the stress response of the MD simulations to the experiments and finite element simulations of single crystal Cu, two main differences need to be addressed: the applied strain rate and specimen size. In the MD simulations, very high strain rates are present because the atomic periods are on the order of femtoseconds in the simulations. Lower applied strain rates lower the magnitude of the stress response due to the lessening of phonon drag (cf. Follansbee [33]).

The specimen size is also expected to change the stress response. Horstemeyer and Baskes showed that at the nanoscale there exists a size dependency; as the size increases, the yield stress decreases. For the MD simulations in this study, the micro/macroyield stresses were 1.95/3.1 GPa in simple shear, 0.47/0.5 GPa for the solid torsion specimen, and 0.2/0.21 GPa for the hollow torsion specimen. The solid torsion experimental values were 3.5/4.8 MPa. Approximately three orders of magnitude difference in the yield stress exists with approximately six orders of magnitude difference in size when comparing the atomistic to experimental results and specimens. Thus a simple square root size scaling is consistent with the observed strength difference. This size scaling is approximately what was found by Horstemeyer et al. [28].

Other experiments qualitatively validate the experimental yield stresses observed in our experiments. Schmid and Boas [14] experimentally showed a microyield stress of 4.5 MPa for single crystal Cu in tension. Phillips [15] performed direct shear on single crystal Cu with different orientations and observed a value of 0.6 MPa for yield. Jackson and Basinski [16] conducted tension tests on single crystal Cu specimens with different crystal orientations and found a range of 0.50–1.24 MPa for the critical resolved shear stress. Honeycombe [17] experimentally showed a critical resolved shear stress of 0.34–0.98 MPa for single crystal Cu depending on the purity level. These values are on the same order as our large scale torsion results. More recently, Quilici et al. [18] obtained a critical resolved shear stress of 0.8 MPa for 1 mm diameter torsion specimens of single crystal Cu.

Even for polycrystalline Cu this size scale trend has been observed. Fleck et al. [34] performed micron scale solid torsion experiments of polycrystalline Cu with different radii. The radii were 12, 15, 20, 30, and 170 μm, and the corresponding yield stresses taken from a 0.2% strain offset were 229, 205, 140, 130, and 120 MPa, respectively. Again, as the size increased, the yield stress decreased.

The much larger value for the MD simulations was expected because of the small size and higher applied strain rate, but this does not address the effect of initial dislocation density. In the MD simulations, a pristine block of material without initial defects was used. In the torsion experiment, the initial defect density was expected to be low because of the method of producing the single crystals, but realistically (though not measured) one would anticipate some dislocations to be present in the material before torsional testing.

Conclusions

In this investigation, we analyzed simple shear and torsion of single crystal copper by employing experiments, molecular dynamics simulations, and finite element simulations. In particular, we focused on micro/macroyield and the kinematic response. Examining samples with aspect ratios of the circumference of the cylinder to the axial gauge length of the torsion specimen equal to the ratio of the length to height in simple shear, we observed an oscillatory deformation pattern in simple shear and torsion that relates to the underlying crystalline nature of discrete slip (plastic spin). The ratio of wave amplitude divided by cylinder circumference in torsion ranged from 0.02–0.06 for the three different methods of analysis: experiments, molecular dynamics simulations, and finite element simulations. For the molecular dynamics and finite element simulation simple shear case, the ratio of wave amplitude divided by the specimen length and ranged from 0.23–0.26. Although each method gave similar results for each type boundary condition, it is clear that the simple shear case resulted in amplitudes that were approximately five times larger than torsion. We attributed this to a different crystalline lattice reorientation torsion (rate) in torsion and simple shear. The simple shear case constrains the dislocation activity to planar double slip but torsion experiences quadruple slip. Finally, we extrapolated the atomistic yield stresses to a much larger scale and these comparisons were close to the experimental data in the literature and in our study.

Acknowledgments

This work has been sponsored by the U.S. Department of Energy, Sandia National Laboratories under contract DE-AC04-94AL85000. MIB would like to acknowledge support from the Office of Basic Energy Sciences, Department of Materials Sciences, in the DOE.

References

[1] Shrivastava, S. C., Jonas, J. J., and Canova, G., 1982, J. Mech. Phys. Solids, **30**(1/2), p. 75.
[2] Johnson, G. R., Hoegfeldt, J. M., Lindholm, U. S., and Nagy, A., 1983, ASME J. Eng. Mater. Technol., **105**, p. 42.
[3] Montheillet, F., Cohen, M., and Jonas, J. J., 1984, Acta Metall., **32**(11), p. 2077.
[4] Canova, G. R., Kocks, U. F., and Jonas, J. J., 1984, Acta Metall., **32**(2), p. 211.
[5] Field, D. P., and Adams, B. L., 1990, ASME J. Eng. Mater. Technol., **112**, p. 315.
[6] Horstemeyer, M. F., and McDowell, D. L., 1998, Mech. Mater., **27**, p. 145.
[7] Khan, A. S., and Parikh, Y., 1986, Int. J. Plast., **2**, p. 379.
[8] Hecker, S. S., Stout, M. G., and Eash, D. T., 1981, Los Alamos Report, LA-UR-81-3447.
[9] Butler, G. C., Graham, S., McDowell, D. L., Stock, S. R., and Ferney, V. C., 1998, ASME J. Eng. Mater. Technol., **120**, p. 197.
[10] Tanner, A. B., and McDowell, D. L., 1999, Int. J. Plast., **15**, p. 375.
[11] Yakou, T., Hasegawa, T., and Karashima, S., 1985, Trans. Jpn. Inst. Met., **26**(2), p. 88.
[12] Franciosi, P., Stout, M. G., O'Rourke, J., Erskine, B., and Kocks, U. F., 1987, Acta Metall., **35**(8), p. 2115.
[13] Khan, A. S., and Wang, X., 1993, Int. J. Plast., **9**, p. 889.
[14] Schmid, E. and Boas, W., 1950, *Plasticity of Crystals*, Hughes, London.
[15] Phillips, W. L., 1962, Trans. Metall. Soc. AIME, **224**, p. 845.
[16] Jackson, P. J., and Baskinski, Z. S., 1967, Can. J. Phys., **45**, p. 707.
[17] Honeycombe, R. W. K., 1984, *The Plastic Deformation of Metals*, Edward Arnold, p. 20.
[18] Quilici, S., Forest, S., and Cailletaud, G., 1998, J. Phys. IV France, **8**, p. 325.
[19] Rashid, M. M., Gray, G. T., and Nemat-Nasser, S., 1992, Philos. Mag. A, **65**(3), p. 707.
[20] Horstemeyer, M. F., McDowell, D. L., and McGinty, R. D., 1999, Modell. Simul. Mater. Sci. Eng., **7**, pp. 253–273.
[21] Foiles, S. M., 1985, Phys. Rev. B, **32**, p. 7685.
[22] Brenner, D. W., 1996, "Chemical Dynamics and Bond-Order Potentials," MRS Bulletin, pp. 36–41.
[23] Stoneham, M., Harding, J., and Harker, T., 1996, "The Shell Model and Interatomic Potentials for Ceramics," MRS Bulletin, Feb. pp. 29–35.
[24] Daw, M. S. and Baskes, M. I., 1984, Phys. Rev., **B29**, p. 6443.
[25] Daw, M. S., Foiles, S. M., and Baskes, M. I., 1993, Materials Science Reports, A Review Journal, **9**, No. 7-8, p. 251.
[26] Angelo, J. E., Moody, N. R., and Baskes, M. I., 1995, Modelling Simul. Mater. Sci. Eng., **3**, p. 289.
[27] Baskes, M. I., Sha, X., Angelo, J. E., and Moody, N. R., 1997, Modelling Simul. Mater. Sci. Eng., **5**, p. 651.
[28] Horstemeyer, M. F., Baskes, M. I., and Plimpton, S. J., 2001, Acta Mater., **49**, p. 4363.
[29] Horstemeyer, M. F., and Baskes, M. I., 1999, ASME J. Eng. Mater. Technol., **121**, p. 114.
[30] Cuitino, A. M., and Ortiz, M., 1992, Modell. Simul. Mater. Sci. Eng., **1**, p. 225.
[31] Hibbitt, Karlsson, and Sorensen, 1998, ABAQUS 5.8.
[32] Boukadia, J., and Sidoroff, F., 1988, Arch. Mech., **40**(5–6), p. 497.
[33] Follansbee, P. S., 1985 *Metallurgical Applications of Shock Wave and High Strain Rate Phenomena*, L. E. Murr, K. P. Staudhammer, and M. A. Meyers, eds. Marcell Dekker, New York, p. 451.
[34] Fleck, N. A., Muller, G. M., Ashby, M. F., and Hutchinson, J. W., 1994, Acta Metall., **42**(2), p. 475.